Received: 14 August 2017 | Revised: 7 November 2018 | Accepted: 14 January 2019

DOI: 10.1002/term.2814

RESEARCH ARTICLE

WILEY

Injectable freeze-dried chitosan-platelet-rich-plasma implants improve marrow-stimulated cartilage repair in a chronic-defect rabbit model

Garima Dwivedi[1] | Anik Chevrier[2] | Caroline D. Hoemann[1,2] | Michael D. Buschmann[1,2]

[1] Biomedical Engineering Institute, Ecole Polytechnique de Montreal, Montreal, Quebec, Canada

[2] Chemical Engineering Department, Ecole Polytechnique de Montreal, Montreal, Quebec, Canada

Correspondence
Michael Buschmann, Chemical Engineering Department, Ecole Polytechnique de Montreal, Montreal, Quebec, Canada.
Email: michael.buschmann@polymtl.ca

Funding information
Ortho Regenerative Technologies Inc; Natural Sciences and Engineering Research Council of Canada; Groupe de Recherche en Sciences et Technologies Biomédicales; Canada Foundation for Innovation; Canadian Institutes of Health Research

Abstract

Bone-marrow stimulation (BMS) improves knee-joint function but elicits incomplete repair. Liquid chitosan (CS)–glycerol phosphate/blood clots have been shown to improve BMS-based cartilage repair. Platelet-rich-plasma (PRP)—a rich source of growth factors and cytokines—improves recruitment and chondrogenic potential of subchondral mesenchymal stem cells. We hypothesised that repair response in a rabbit chronic-defect model will improve when freeze-dried CS/PRP is used to augment BMS. Bilateral trochlear defects created in New Zealand white rabbits were allowed to progress to a chronic stage over 4 weeks. Chronic defects were debrided and treated by BMS in second surgery, then augmented with PRP (BMS + PRP) or freeze-dried CS/PRP implants (BMS + CS/PRP). The quality of 8-week repair tissue was assessed by macroscopic, histological, and micro computed tomography (Micro-CT) analysis. ICRS macroscopic scores indicated fibrocartilaginous or fibrous repair in control defects that were improved in the BMS + CS/PRP group. An overall improvement in repair in BMS + CS/PRP group was further confirmed by higher O'Driscoll scores, %Saf-O and %Coll-II values. Micro-CT analysis of subchondral bone indicated ongoing remodelling with repair still underway. Quality and quantity of cartilage repair was improved when freeze-dried CS/PRP implants were used to augment BMS in a chronic defect model.

KEYWORDS

augmentation, cartilage repair, chitosan, chronic model, marrow stimulation, platelet-rich plasma

1 | INTRODUCTION

Bone-marrow stimulation (BMS) is a purely surgical process, which initiates cartilage repair by fracturing or drilling into subchondral bone. BMS procedures initiate the formation of a blood clot around fractured bone followed by migration of subchondral progenitor cells, which differentiate into a chondrogenic phenotype to form a repair tissue with variable amounts of hyaline and fibrous cartilage (Shapiro, Koide, & Glimcher, 1993). The repair tissue is typically characterised by low quality and compromised durability, and larger lesions in older patients are even more challenging to treat.

One possible reason for the poor performance of BMS is that the blood clot rapidly shrinks to a fraction of its initial size due to platelet-mediated clot retraction, resulting in lack of defect filling and possible detachment from the tissue surface. One way to prevent clot retraction is to add chitosan (CS), a polymer of glucosamine and N-acetyl glucosamine units, to the blood (Hoemann et al., 2007). Liquid CS-glycerol phosphate (GP)/blood implants can be applied over BMS-treated cartilage defects where they coagulate in situ and inhibit platelet-mediated clot retraction leading to the formation of a voluminous, adherent, and physically stable clot with access to underlying marrow (Hoemann et al., 2005). When used in conjunction with

BMS procedures, CS-GP/blood implants promote cell recruitment, transient vascularisation, and subchondral bone remodelling leading to integrated repair and increased hyaline character of the repair tissue (Hoemann et al., 2005; Chevrier, Hoemann, Sun, & Buschmann, 2007; Hoemann et al., 2007; Chen et al., 2011). These implants were tested clinically (Shive et al., 2015; Stanish et al., 2013) and have now been approved in several countries to treat cartilage lesions (BST-CarGel®, Smith & Nephew, Memphis, TN). One drawback of this technology is that liquid-CS solutions have limited stability during storage due to acid hydrolysis of CS and loss of viscosity (Varum, Ottoy, & Smidsrod, 2001). A freeze-dried form of CS would not only overcome this limitation by increasing stability and shelf life but also permit easier sterilisation.

A microenvironment stimulating chondrogenic differentiation of bone marrow-derived stromal cells (BMSCs) may be achieved by addition of platelet-rich plasma (PRP) to the defect milieu. PRP is prepared by sequential centrifugation of whole blood and is a rich source of growth factors and cytokines such as platelet-derived growth factor (PDGF), vascular endothelial growth factor (VEGF), insulin-like growth factor (IGF), and epidermal growth factor (EGF), which play an important role in inflammatory and wound-repair phenomena (Gonshor, 2002; Marx, 2001; Marx et al., 1998). Earlier studies have shown that PRP can induce a significant improvement in BMSC recruitment, angiogenesis (Simpson, Mills, & Noble, 2006; Veillette & McKee, 2007), expression of cartilage matrix (Smyth, Murawski, Fortier, Cole, & Kennedy, 2013), proliferation, and viability of chondrocytes and BMSCs (Lee, Park, Joung, Park, & Do, 2012; Park, Lee, Kim, Ahn, & Do, 2012) as well as stimulate migration and chondrogenic potential of subchondral BMSCs (Kruger et al., 2012). A strong influence of properties and potential of bone-marrow-derived stem cells in influencing cartilage repair has been demonstrated in the earlier studies (Dwivedi, Chevrier, Alameh, Hoemann, & Buschmann, 2018; Dwivedi, Chevrier, Hoemann, & Buschmann, 2018). Using an ovine chronic-defect model, Milano et al showed that when used as an adjunct to BMS, PRP enhanced the repair response versus BMS alone (Milano et al., 2010). Although the application of PRP improved the macroscopic and mechanical outcome, the hyaline nature of the repair tissue was still lacking. The efficacy of PRP in improving cartilage repair has been questioned due to multiple studies reporting less positive results in animal models (Brehm et al., 2006; Kon et al., 2010). We believe that inferior outcome with PRP could arise from the poor stability of PRP clots in vivo, which is even more pronounced than blood clots (Chevrier et al., 2017). Combination of PRP with CS may help in overcoming this limitation thereby increasing residency and bioactivity of PRP.

Progression to advanced stages of osteoarthritis (OA) may be prevented by early diagnosis and treatment. However, in cartilage lesions that are asymptomatic for longer times (Bredella et al., 1999; Hardaker, Garrett, & Bassett, 1990), BMS may have more severe limitations and therefore be less effective in treating older, chronic, and extensive lesions. Chronic defects may alter joint homeostasis resulting in less favourable clinical outcomes (Bouwmeester, Kuijer, Homminga, Bulstra, & Geesink, 2002; Bouwmeester, Kuijer, Terwindt-Rouwenhorst, van der Linden, & Bulstra, 1999; Hunziker, 1999). To better represent this clinical situation, we developed a preclinical model to simulate degenerated chronic defects and examine the potential of BMS combined with CS/PRP in improvement of cartilage regeneration in chronic defects that are more challenging than acute lesions. It is already known that osteochondral defects smaller than 3 mm in young rabbits possess the potential for spontaneous regeneration (Mizuta, Kudo, Nakamura, Takagi, & Hiraki, 2006), and several studies have reported a period of approximately 1 month to be adequate for development of chronic defect model in small animals (Harada et al., 2015; Hepp et al., 2009). Accordingly, we used skeletally mature rabbits with a defect size of 4 × 4 mm developed to chronicity over a period of 4 weeks. With these aspects in mind, we carried out this study to test the hypothesis that augmentation of BMS with freeze-dried CS/PRP implants (BMS + CS/PRP) would improve repair response in a rabbit chronic-defect model compared with BMS augmented with recalcified PRP (BMS + PRP).

2 | MATERIALS AND METHODS

2.1 | Preparation of freeze-dried CS formulation and PRP isolation

Freeze-dried CS cakes consisted of 0.56% (*w*/vol) CS with 1% (*w*/vol) trehalose and 42.2-mM calcium chloride. To prepare, 0.056-g CS (number average molar mass M_n 36.6 kDA and 80.2% DDA, produced in-house and characterised with NMR spectroscopy, Lavertu et al., 2003, and size-exclusion chromatography/multiangle laser-light scattering, Nguyen, Winnik, & Buschmann, 2009) was mixed with 7.69-g water and 156 µl of 1 N HCl. Following overnight mixing, 1.56 ml of 3% (*w*/w) $CaCl_2$ and 666 µl of 15% (*w*/*v*) trehalose solutions were added, and the final solution was sterilised by filtration. Finally, 300-µl aliquots were prepared in 2-ml sterile glass vials and freeze-dried using the following conditions: (a) ramped freezing to −40°C in 1 hr then isothermal 2 hr at −40°C, (b) −40°C for 48 hr at 100 mTorr, and (c) ramped heating to 30°C in 12 hr then isothermal 6 hr at 30°C, at 100 mTorr.

Autologous PRP was generated by sequential centrifugation of citrate-anticoagulated whole blood. Approximately 9 ml of autologous blood was extracted from rabbit and mixed with 1 ml of 3.8% (*w*/vol) sodium citrate before further processing. The whole blood was centrifuged at 160 g for 10 min. Following collection of the supernatant in addition to approximately the first 1–2 mm of erythrocytes, a second centrifugation was carried out at 400 g for 10 min. Bottom 1.5-ml fraction containing PRP was isolated. Complete blood counts revealed that, on average, the ratio of platelets, leukocytes, and erythrocytes in isolated PRP versus whole blood was 3×, 1×, and 0.1×, respectively, which makes this a leukocyte-rich PRP.

2.2 | Experimental design and rabbit surgical model for cartilage repair in chronic lesions

Canadian Council on Animal Care guidelines were observed and research protocol was approved by an institutional ethics committee

for animal research. Using skeletally mature female New Zealand white rabbits, the chronic-defect model was first validated in a pilot study utilising a small number of animals (n = 3) and short duration (4-week development to chronicity followed by 3-week repair). The small number of animals was chosen because this was the preliminary study carried out to assess the feasibility of development of chronicity in the model, a relatively new approach, before progressing with the more comprehensive study. The pilot study was used to characterise and compare fresh defect (n = 2 knees), 4-week-old chronic defects and repair response in 4-week-old chronic defects (n = 2 knees) treated with BMS alone (BMS + PRP, n = 1 knee) or BMS augmented with 1% (w/v) CS/PRP implants (BMS + CS/PRP, n = 1 knee) for 3 weeks. PRP controls were not included in this pilot study because the aim was to validate the chronic model rather than study the effect of treatments (Figure 1).

Once the results from the pilot study were analysed, a larger group (n = 8) of skeletally mature (8–9 months old) female New Zealand white rabbits were then used in a bilateral model that limits the influence of interanimal variation via a contralateral control (Figure 1). Two surgeries were performed to assess the development and repair of chronic cartilage defects. Following induction with xylazine-ketamine, animals were maintained under general anaesthesia using isofluorane-oxygen. Bilateral, parapatellar arthrotomies were performed to expose the synovial joint. Full-thickness chondral lesions measuring 4 × 4 mm were created in the trochlear central groove by scraping with 1.5- and 2.75-mm flat surgical blades taking care not to remove calcified cartilage. Knees were closed in sutured layers (Figure 2a,b). A period of 4 weeks was allowed for the defects to progress to chronic defect stage (Figure 2c,d). Four weeks after the defects were created in the first surgery, a second surgery was performed, and original lesion was identified. Calcified cartilage (CC) and repair tissues (when present) were completely debrided using a flat blade to expose the underlying subchondral bone, without damaging the subchondral bone plate. Using a high-speed microdrill, four subchondral perforations measuring 0.9 mm diameter and 6 mm deep were made on each trochlear defect in both knees, similar to what was done previously by our group in acute models (Chen et al., 2011; Chen et al., 2013; Figure 2e,f). Constant cooling irrigation was applied for removal of loose bone debris and prevention of heat necrosis (Chen et al., 2009). The defect on one knee received treatment with one drop of CS/PRP mixture. Immediately before implantation, the CS cake (300 µl) was solubilised with 300 µl autologous PRP (Figure 2g). One drop of CS/PRP was applied to the drilled trochlear defect using a 1-ml syringe and 18-gauge needle. The contralateral defect was treated with one drop of PRP recalcified with 42.2mM calcium chloride (Figure 2h). In both cases, knees were closed 5 min post application. The treatments were alternated between right and left knees. The patella was repositioned, and knee was closed in sutured layers. No perioperative antibiotics were administered after either surgery, but animals received extended analgesia with a fentanyl transdermal patch. Knees were allowed unrestricted motion and constantly monitored for infections and other complications following both surgeries. Animals were sacrificed 8 sweeks after second surgery, and knees were harvested for comparison of 8-week repair response initiated by marrow stimulation in presence of CS/PRP (BMS + CS/PRP group, n = 8 knees) and recalcified PRP (BMS + PRP group, n = 8 knees).

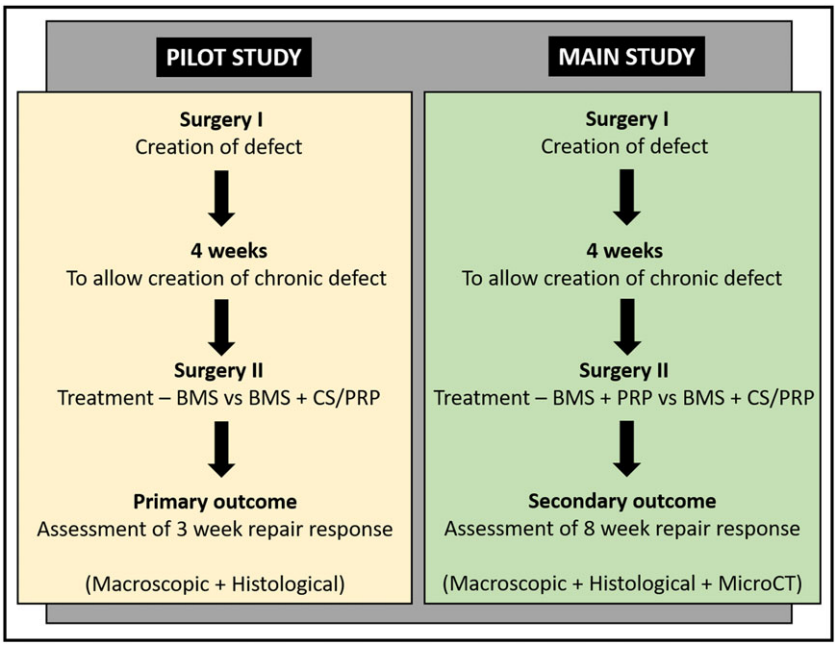

FIGURE 1 Timeline of the stages in the pilot and main study. Two surgeries were performed. The defect was created in the first surgery and treated in the second surgery. A time period of 4 weeks was chosen to allow the defects to progress to chronic stage between creation of defects and second surgery for treatment. The pilot study used three animals where the defects were created in first surgery. The defects were left without any further manipulation for 4 weeks to progress to chronic stage. In the second surgery, the defects were either left as such, or treated with bone-marrow stimulation alone (BMS) or bone-marrow stimulation + chitosan (CS)– platelet-rich-plasma (PRP) implants (BMS + CS/PRP). The animals were sacrificed 3 weeks after the second surgery to assess the 3-week repair in order to gain mechanistic insight into the early events in cartilage repair initiated by CS/PRP. Eight animals were used in the main study. The events in the main study were same as pilot study with a few exceptions. BMS + CS/PRP group was compared with BMS + PRP group. The repair was investigated 8 weeks after the second surgery [Colour figure can be viewed at wileyonlinelibrary.com]

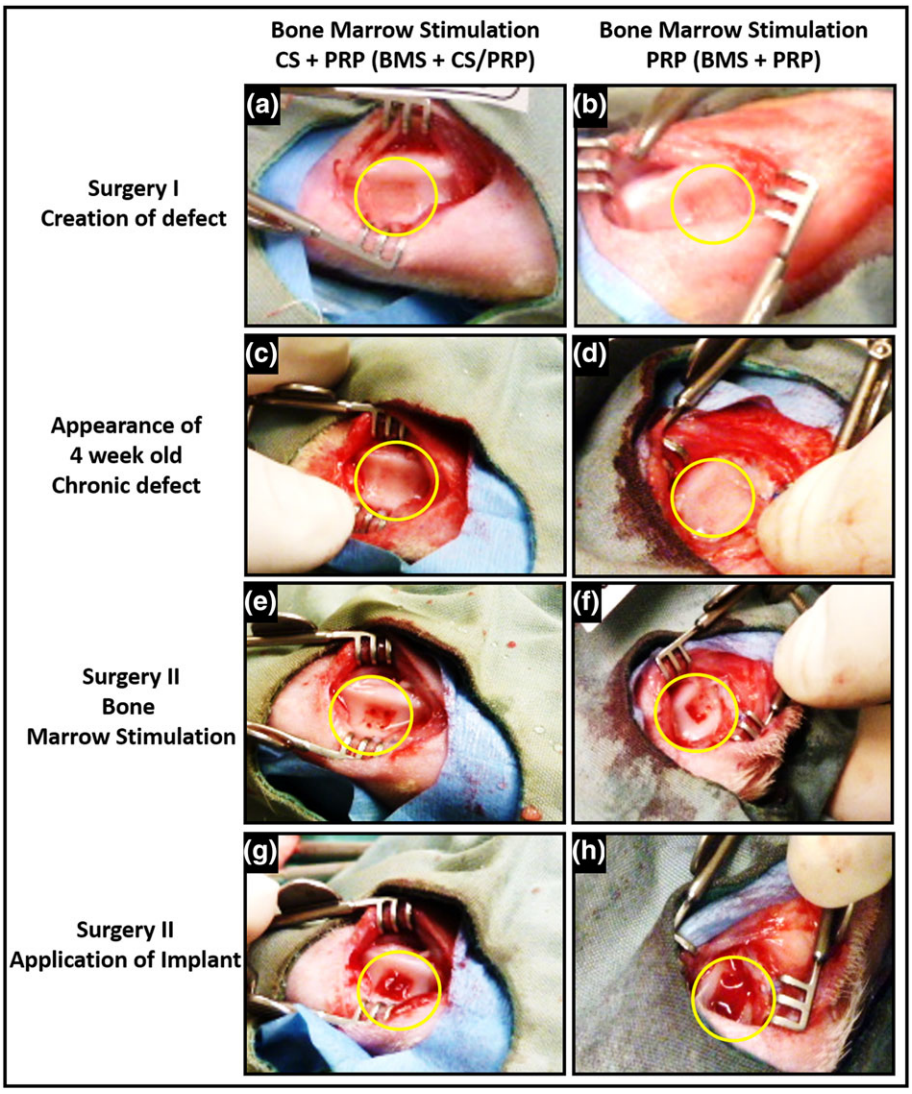

FIGURE 2 Procedure of surgical manipulation to create and treat chronic defects using bone-marrow stimulation + chitosan (CS)/ platelet-rich-plasma (PRP) implants (left panels) or BMS + PRP (right panels). (a,b) Creation of 4 × 4 mm defects by debriding all non-calcified cartilage from trochlea; (c,d) appearance of chronic defects 4 weeks after creation at the time of second surgery; (e,f) treatment of defects by debriding spontaneous repair tissue (when present) and calcified cartilage and drilling four holes measuring 0.9 mm in width and 6-mm deep; (g) application of CS/PRP implant at defect site; (h) application of recalcified PRP at defect site [Colour figure can be viewed at wileyonlinelibrary.com]

2.3 | Characterisation of repair

Animals were sacrificed by overdose of pentobarbital and femoral ends were fixed in 4% paraformaldehyde/1%glutaraldehyde/0.1 M Sodium cacodylate (pH 7.3). Low-magnification images of fixed repair tissues were obtained with a dissection microscope equipped with digital camera to determine their gross structure and appearance using Northern Eclipse software (Empix Imaging). Images of repair tissues were scored by two independent, blinded readers using the International Cartilage Repair Society (ICRS) macroscopic scoring system, 0 (*severely abnormal*) to 12 (*for normal*; van den Borne et al., 2007). Scores from two readers were averaged and used as an indicator of gross pathology of repair tissues.

Samples were decalcified in Ethylenediaminetetraacetic acid (EDTA) with trace paraformaldehye and embedded in optimum cutting temperature compound (OCT), and transverse sections were obtained from three levels: from the middle of the proximal and distal holes and from between holes. Sections were stained with Safranin O/Fast Green and scanned using a Nanozoomer RS system (Hamamatsu, Japan). Repair tissue was defined as all nonmineralised tissue above the subchondral bone plate. Digital Saf-O stained sections were scored by two independent, blinded observers using a previously published O'Driscoll histological scoring method—ranging from 0 (worst tissue quality) to 27 (*best tissue quality*)—modified to assess subchondral bone health by an additional three-point value (Chen et al., 2011). Each Saf-O-stained section was assessed for 10 criteria (Figure 6m) to evaluate quality of repair tissue in addition to health of adjacent cartilage and subchondral bone repair. The scores obtained from three sections were averaged for both readers and used for assessment of quality of fill in defects (ICC of 0.86 for total O'Driscoll score for both readers).

Sections collected from each defect were also used to determine %Saf-O and %Coll-II in the chondral repair tissue using a previously described method (Hoemann et al., 2015). Briefly, soft repair tissues were cropped by identifying projected articular surface and tidemark with the help of flanking articular cartilage and accounting for the curvature of the trochlear groove. Only the soft repair tissue above the tidemark was used to determine hue–saturation–value threshold limits for Saf-O and Coll-II. %Saf-O and %Coll-II positive regions of repair tissues were measured using in-house Matlab routine software.

2.4 | Micro-CT analysis of subchondral bone repair

Micro-CT scanning of fixed femur ends was done to characterise subchondral bone repair and remodelling (Skyscan x-ray microtomography 1172, Kontich, Belgium). Femurs were scanned with an aluminium filter at 14.1μM pixel-size resolution with an X-ray source voltage of 56 kV, 1,180 BMSec exposure, 0.45 rotation steps, and three averaging frames. Trochlear micro-CT image stacks were first reconstructed with NRecon software 1.6.1.5 using the following parameters: smoothing of 2, ring artifact reduction of 10, beam-hardening correction of 40%. Datasets were repositioned with DataViewer software 1.4.3, and region of interest were applied followed by 3D micro-CT analysis. The regions of interest were of the rectangle adapted surface type (Marchand, Chen, Buschmann, & Hoemann, 2011) and measured 3 × 3 × 2 mm (Figure S1). Bone-morphometric parameters were calculated including bone-surface density (BS/TV), bone surface (BS), bone volume (BV), porosity, connectivity density, and number and thickness of trabeculae by using the global-thresholding procedure in CTAn software (version 1.9.3.0, Skyscan, Kontich, Belgium).

2.5 | Statistical analysis

Statistical analyses were performed using SAS Enterprise Guide 7.1 and SAS 9.4. Because several sections were collected from both legs of each rabbit, a mixed model was used to account for the influence of donor. Fixed effects were treatments (BMS + PRP, n = 8 knees and BMS + CS/PRP, n = 8 knees), whereas donor was a random effect. Data in figures are presented as mean (diamond); median (line); Box: 25th and 75th percentile; Whiskers: Box to the most extreme point within 1.5 interquartile range. $p < 0.05$ was considered statistically significant.

3 | RESULTS

3.1 | Freeze-dried CS/PRP implants applied in the pilot study induced inflammatory and wound-bloom repair responses in chronic cartilage defects

Chronic defects analysed from the pilot study were noticeably distinct from the fresh defects (Figure 3a) or surrounding healthy tissue after 4 weeks of defect creation (Figure 3b). Residual calcified cartilage along with spontaneous repair response arising from the bone was occasionally observed (Figure 3f,j. Although debridement appeared to have preserved the calcified cartilage intact due to absence of any punctuate bleeding at the time of initial surgery (Figure 2a), the histological examination of Saf-O stained transverse sections of fresh defects showed that calcified cartilage had been partly debrided (Figure 3e,i). The chronic defect showed signs of inflammatory response, and the base of the defect was soft to touch suggesting reduced bone-mineral density—expected event in early disease pathogenesis. Complete debridement down to subchondral bone was performed prior to BMS (Figure 2e,f) and application of either CS/PRP (Figure 2g) or recalcified PRP (Figure 2h).

Four-week-old chronic defects treated with BMS + CS/PRP showed incomplete repair 3 weeks after implantation (Figure 3c). Histological examination of Saf-O-stained transverse sections taken through holes revealed depressed repair tissues and enlarged remodelling drill holes (Figure 3g,k), reminiscent of a wound-bloom repair response (Guzman-Morales, Lafantaisie-Favreau, Chen, & Hoemann, 2014). Drill holes were devoid of subchondral cartilage and mostly filled with a polymorphonuclear cell-rich granulation tissue, where neutrophils colocalised with CS (Figure 3g,k). Contralateral 4-week-old chronic defects treated with BMS alone also demonstrated incomplete repair 3 weeks after treatment (Figure 3d), Histological examination showed fibrocartilaginous and endochondral ossification repair responses, associated with chondrocyte hypertrophy and vascular invasion (Figure 3h,l).

3.2 | Freeze-dried CS/PRP implants solidified quickly in situ and improved the macroscopic repair appearance in chronic defects at 8 weeks after implantation

Clear differences in the solidification and stability of implants were observed at the time of surgery. On average, CS/PRP implants solidified in situ within 30–60 s. In contrast, in most cases, recalcified PRP implants did not coagulate even after passage of 5 min. In general, assessment of 8-week-repair outcome was found to be generally poor (Figure 4a–d), most likely due to the chronic nature of the current defects. Incomplete fill and poor repair-tissue integration to adjacent cartilage tissue were observed in both groups (Figure 4). Defect surfaces were significantly depressed with irregular surface (Figure 4). Appearance of repair tissues varied from dense white, glossy to reddish, spongy, or tufty (Figure 4). Although higher for BMS + CS/PRP group (mean score 4.75 ± 2.25) compared with BMS + PRP group (mean score 3.25 ± 2.05), macroscopic ICRS scores did not show a significant difference between treatments (p = 0.16; Figure 4e).

However, the BMS + CS/PRP group had the only instance of a nearly normal (Grade II) repair response and only two severely abnormal (Grade IV) repair outcomes, whereas the BMS + PRP group had four instances each of abnormal (Grade III) and severely abnormal (Grade IV) outcomes (Table 1).

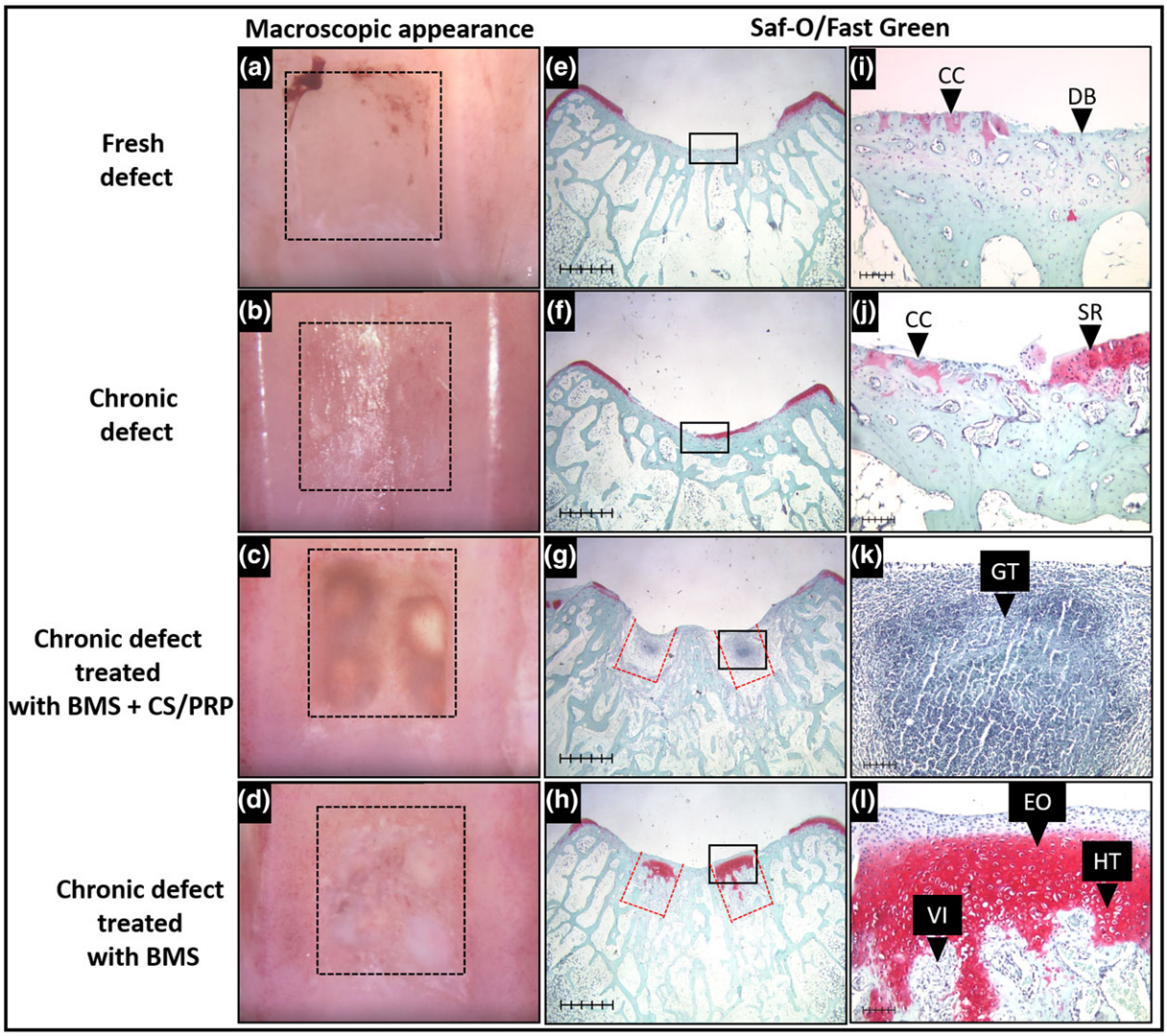

FIGURE 3 Assessment of 3-week repair outcome in pilot study (a, e, i) macroscopic (a) and histopathological assessment (e, i) of fresh defect. Debridement was not homogenous and varying levels of calcified cartilage (CC) and debrided bone (DB) were seen in freshly debrided defects (e, i). (b, f, j) Macroscopic (b) and histopathological assessment (f, j) of chronic defect after allowing 4 weeks for the defect to progress to chronic stage. After 4 weeks, chronic defects showed evidence of partial spontaneous repair (SR) in some areas along with tufts of calcified cartilage (CC; f, j). (c, g, k) Four-week-old chronic defect treated with bone-marrow stimulation (BMS) + chitosan (CS)/ platelet-rich-plasma (PRP) implant for 3 weeks. Granulation tissue formation (GT) and enlarged drill holes were seen in presence of CS/PRP implants (g,k) at 3 weeks after treatment with CS/PRP implants. Red dotted lines in g and h represent original drill holes–hole enlargement and wound-bloom effect is apparent in defect treated with BMS + CS/PRP (g). (d, h,l)—Four week old chronic defect treated with BMS alone for 3 weeks. Fibrocartilagenous repair and endochondral ossification (EO) process were seen in presence of BMS alone, associated with chondrocyte hypertrophy (HT) and vascular invasion (VI). Scale bar (e–h):1 mm, (i–l): 100 μm [Colour figure can be viewed at wileyonlinelibrary.com]

3.3 | Histological assessment showed superior repair in chronic defects treated with freeze-dried CS/PRP implants at 8 weeks after implantation

Higher expression of GAGs and Type 2 collagen was observed in defects with the best histological scores (Figure 5a,b,i,j,e,f,m,n), compared with defects with lowest scores (Figure 5 c,d,k,l,g,h,o,p). Where present, repair tissues showed good integration to underlying bone, although bonding with adjacent cartilage was poor in both groups (Figure 5). Quantitative histomorphometry revealed a significant increase in Type 2 collagen staining in repair tissue matrix for BMS + CS/PRP group (mean 57.37 ± 12.43) compared with BMS + PRP group (mean score 32 ± 15.94), indicating a more hyaline repair (p = 0.003; Figure 5r). Safranin O staining was less widespread than Type 2 collagen staining (Figures 5,6). A higher proportion of repair tissue was glycosaminoglycans (GAG) positive in the BMS + CS/PRP group (mean 44.9 ± 16.3) compared with BMS + PRP group (mean 34.6 ± 8.9), although this result was not significant (p = 0.07; Figure 5q).

Restoration of surface, structural integrity, and thickness were all improved by BMS + CS/PRP treatment (p = 0.05, p = 0.0001, and p = 0.002, respectively; Figure 6a, c vs. b, d and Figure 6l). Margins of defects were recognisable, and degenerative changes were

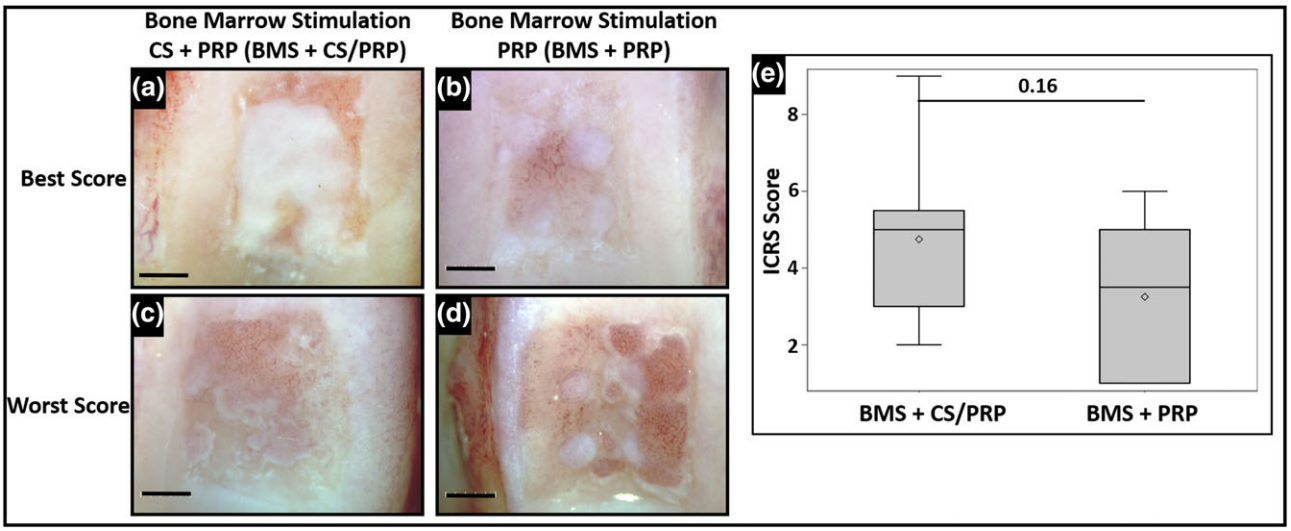

FIGURE 4 Assessment of 8-week repair outcome—Best (a,b) and worst (c,d) repair response in 4 week old chronic defects treated with bone-marrow stimulation (BMS) + chitosan (CS)/ platelet-rich-plasma (PRP); a,c) and BMS + PRP (b,d) after 8 weeks. Scale bar = 1 mm. (e) Mean macroscopic ICRS score was higher (nonsignificant) in defects treated with BMS + CS/PRP versus defects treated with BMS + PRP [Colour figure can be viewed at wileyonlinelibrary.com]

TABLE 1 Number of defects in each repair category for both treatments. Macroscopic repair scored according to the ICRS system

Grade of repair	BMS + CS/PRP	BMS + PRP
I (12-Normal)	0	0
II (8–11 Nearly Normal)	1	0
III (4–7 Abnormal)	5	4
IV (1–3 Severely Abnormal)	2	4

observed in the adjacent cartilage, especially in the BMS + PRP group (p = 0.004; Figure 6 e vs. f). Hypocellular tissue was less frequently observed in BMS + CS/PRP group and incidence of chondrocyte clustering was more frequent in the BMS + PRP group (p = 0.002 and p = 0.009, respectively; Figure 6 g, i vs. h,j). Zonal organisation and tidemark were not restored in any defect at this 8-week time point (Figure 6). One case of a cleft communicating with subchondral cyst was observed in both groups (data not shown). Taken together, mean O'Driscoll score was significantly higher for BMS + CS/PRP group (mean score 20.5 ± 1.69) versus BMS + PRP group (mean score 14.75 ± 1.75; p = 0.0002), indicating superior quality of repair in presence of CS/PRP implants (Figure 6k).

3.4 | Freeze-dried CS/PRP-implants-induced subchondral bone remodelling in BMS-treated chronic defects in 8 weeks after implantation

In both groups at 8-weeks post operative, subchondral bone underneath cartilage defects showed evidence of ongoing remodelling indicating repair was still underway (Figure 5). Quantitative 3-D micro-CT analysis revealed high interindividual variability in bone-structural parameters, and no significant difference between treatments (Figure S1). However, the values for bone-surface density, BS, connectivity density, and trabecular number were all higher for BMS + CS/PRP group compared with BMS + PRP group (all p = 0.01), indicating that CS/PRP implants increased bone remodelling (Figure S1).

4 | DISCUSSION

A chronic model was developed to test the efficacy of CS/PRP implants in augmenting marrow-stimulated repair. Although chronic defects were found to be more challenging to treat than acute defects, CS/PRP implants improved the quality of repair tissues, which suggests that they would constitute a promising approach for treating chronic, degenerated lesions in older patients. Taken together, our data shows superiority of BMS + CS/PRP in repair of chronic defects compared with BMS + PRP, thereby affirming our starting hypothesis.

The chronic-defect model used here was intended to approach the degenerative and inflammatory processes concomitant with metabolic alterations in early OA due to cartilage injury. In line with this, we found that BMS by drilling to 6 mm induced much poorer repair in trochlear chronic defects than in similar acute defects in the rabbit model (Chen et al., 2011; Chen et al., 2013). Recent studies have reiterated the chronic-defect model to be more suitable to study pathogenesis of OA, which is associated with multiple changes in the defect milieu with severe bearing on downstream repair processes. Altered joint homeostasis in old defects has been associated with inferior repair (Saris, Dhert, & Verbout, 2003). The difficulty in treating chronic defects has been recognised in multiple studies in the past (Saris et al., 2003; Verbruggen et al., 2007). Saris et al showed that

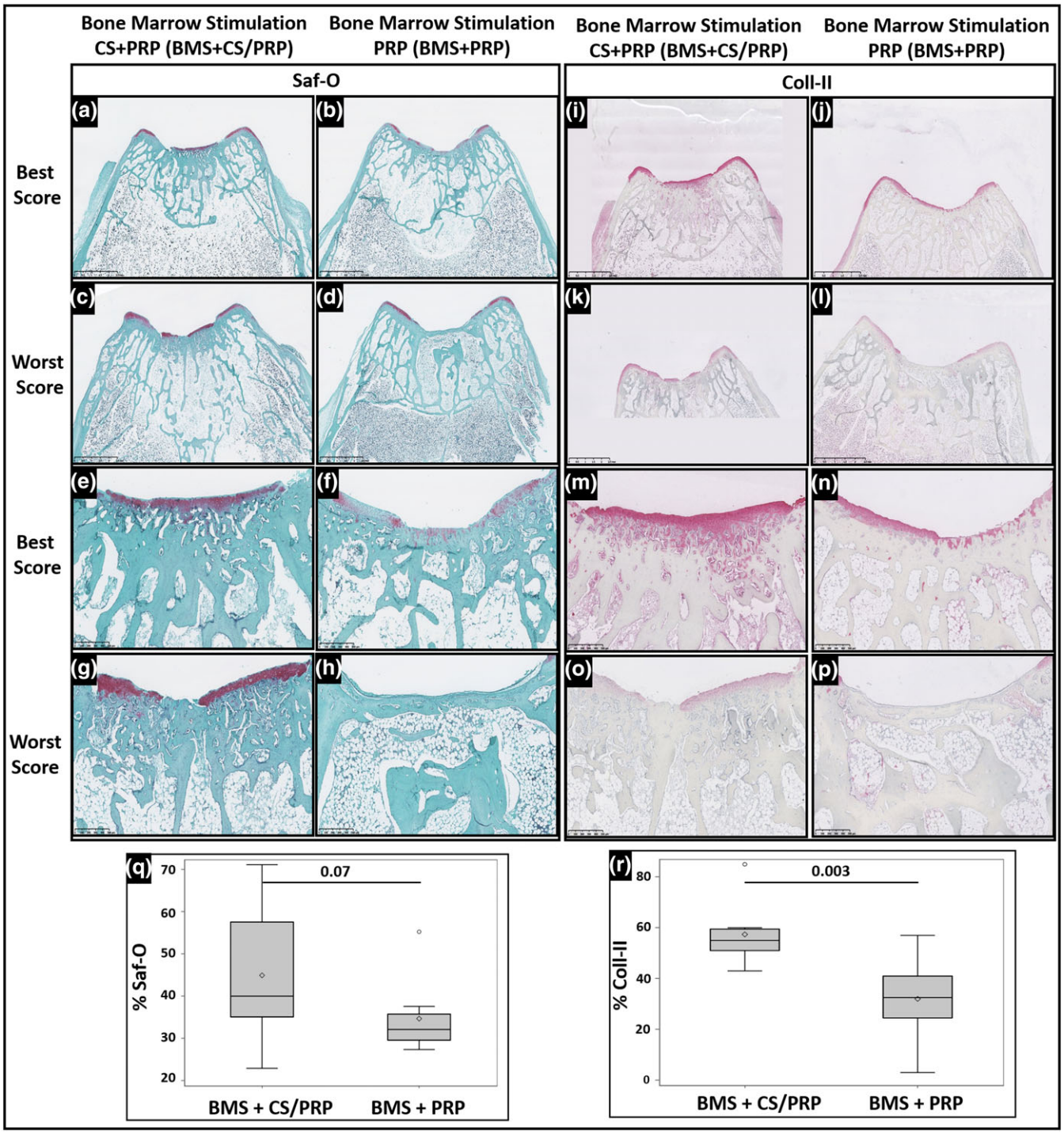

FIGURE 5 Assessment of 8-week repair outcome - Comparison of histopathological assessment of best and worst repair tissues generated in 4 week old chronic defects by bone-marrow stimulation (BMS) + chitosan (CS)/ platelet-rich-plasma (PRP) and BMS + PRP 8 weeks after repair. (a–h) Saf-O staining for best (a,b,e,f) and worst (c,d,g,h) repair outcomes; (i–p) Coll-II immunostaining for best (i,j,m,n) and worst (k,l,o,p) repair outcomes; scale bars 2.5 mm (a–d and i–l) and 500 μm (e-h & m-p). (q) Mean % Saf-O was higher for repair tissues in defects treated with BMS + CS/PRP versus defects treated with BMS + PRP, although this difference was not significant. (r) Mean %Coll-II was significantly higher for repair tissues in defects treated with BMS + CS/PRP versus defects treated with BMS + PRP [Colour figure can be viewed at wileyonlinelibrary.com]

cartilage repair outcome in groups receiving late treatment was significantly inferior compared with early treatment group and was comparable with untreated group (Saris et al., 2003). Rodrigo et al suggested that synovial fluid may have a stimulatory effect in treatment of acute defects although may be inhibitory in chronic defect treatment (Rodrigo, Steadman, Syftestad, Benton, & Silliman, 1995).

PRP is a rich source of growth factors and cytokines, which play important roles in inflammatory and wound repair phenomena

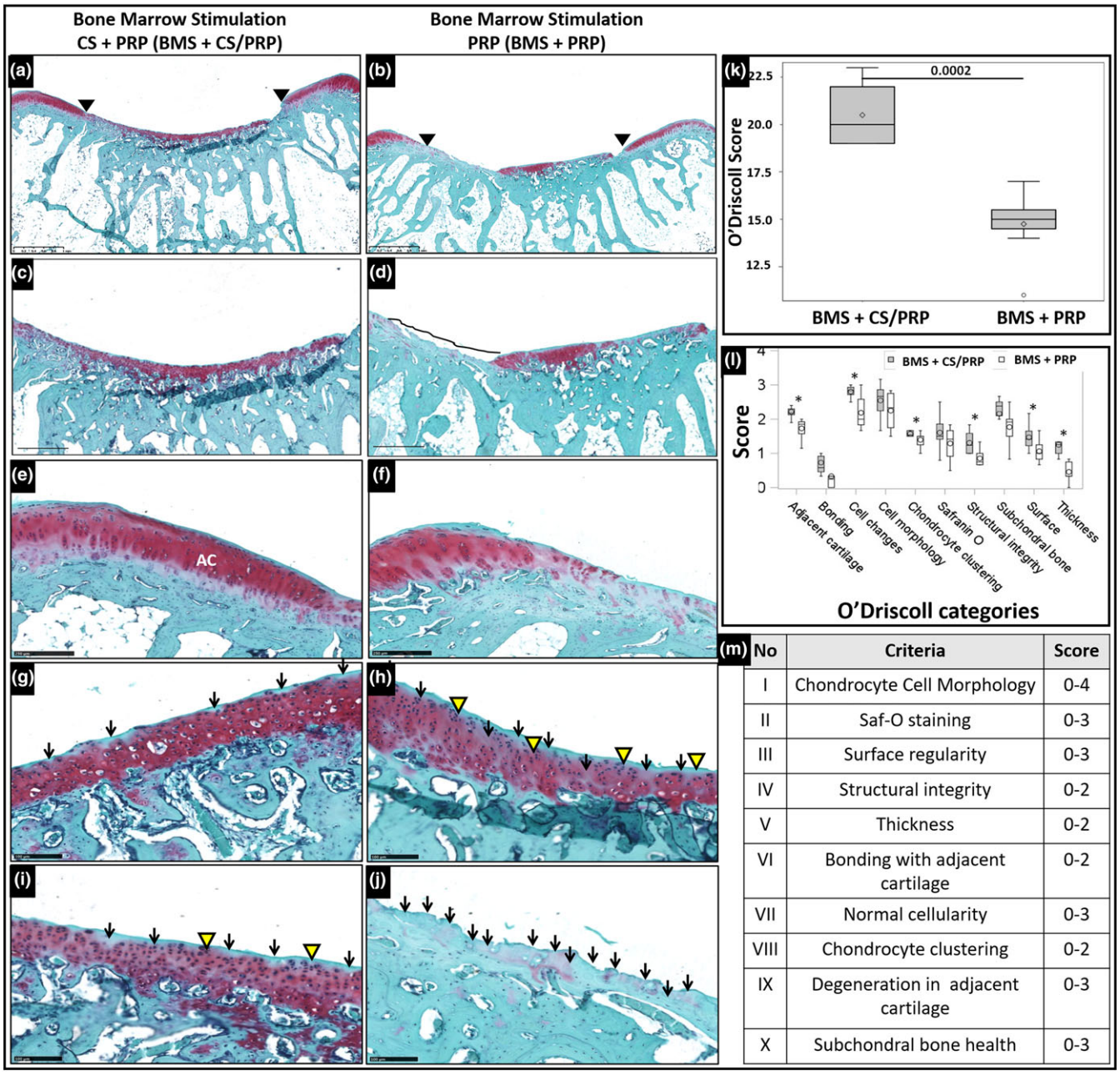

(m)

No	Criteria	Score
I	Chondrocyte Cell Morphology	0-4
II	Saf-O staining	0-3
III	Surface regularity	0-3
IV	Structural integrity	0-2
V	Thickness	0-2
VI	Bonding with adjacent cartilage	0-2
VII	Normal cellularity	0-3
VIII	Chondrocyte clustering	0-2
IX	Degeneration in adjacent cartilage	0-3
X	Subchondral bone health	0-3

FIGURE 6 Assessment of 8-week repair outcome—representative sections of repair tissues of 4-week-old chronic defects generated 8 weeks after treatment with bone-marrow stimulation (BMS) + chitosan (CS)/ platelet-rich-plasma (PRP) and BMS + PRP. (a, b) Restoration of surface and structural integrity was better in presence of CS/PRP (a) versus PRP (b) (defect margins flanked by solid black arrows); (c, d) Missing repair tissue (line) in BMS + PRP (d) versus more uniform tissue in BMS + CS/PRP (c); (e, f) Comparison of adjacent cartilage (AC) showing improved appearance in the case of BMS + CS/PRP; (g, h) best sections, (i, j) worst sections–all sections from same animal. Black arrows indicate zones of hypocellularity, yellow arrows indicate cell clusters, both more frequent in BMS + PRP. Scale bars = a,b: 1 mm, e-f: 250 µm, (g–j) 100 µm. (k) Mean O'Driscoll score was significantly higher for repair tissues in defects treated with BMS + CS/PRP versus defects treated with BMS + PRP. (l) Significant differences (*) were observed between treatments, and scores for adjacent cartilage (p = 0.004), cellular changes (p = 0.002), cell clusters (p = 0.009), structural integrity (p = 0.0001), surface integrity (0.05), and thickness of repair tissue (p = 0.002) were significantly higher for defects treated with BMS + CS/PRP. (m) Criteria used in modified O'Driscoll scoring with respective score range [Colour figure can be viewed at wileyonlinelibrary.com]

(Gonshor, 2002; Marx et al., 1998). Although the exact mechanism of PRP action has not been understood, BMSC recruitment, expression of cartilage matrix (Milano et al., 2010) in addition to migration, proliferation, and chondrogenesis of subchondral BMSCs have been shown to be positively influenced by PRP. In contrast, some studies report that PRP exerts a stimulatory effect on proliferation of chondrocytes and BMSCs but has no effect on their chondrogenic differentiation (Drengk, Zapf, Sturmer, Sturmer, & Frosch, 2009; Gaissmaier et al.,

2005; Kaps et al., 2002; Kruger et al., 2012). Reduced expression of lineage-specific markers was observed in cells expanded in the presence of PRP (Li et al., 2013). Therefore, we believe that BMS augmented with recalcified PRP was an appropriate baseline treatment to be compared with BMS-repair outcome elicited in presence of CS/PRP implants. Our results indicate insufficient capability of PRP in enabling cartilage healing in a chronic defect. Similarly, in a previously published study, PRP was unsuccessful in regenerating the hyaline nature of repair tissue in a chronic defect treated with BMS (Milano et al., 2010). In our study, PRP failed to solidify even after several minutes in most cases, suggesting impaired in vivo residency of a liquid implant and providing a possible mechanism for reduced efficacy of PRP in cartilage regeneration. In our recent study, CS/PRP clots showed significant increase in viscosity vs PRP and reduced clotting time by four times compared with recalcified PRP (Chevrier et al., 2017). Whereas CS/PRP clots remained voluminous even 1 hr after clotting, recalcified PRP clots had lost ~80% of their original volume as a result of serum exudation (Chevrier et al., 2017). The resulting quick loss of platelet-derived bioactive factors could potentially limit repair in these defects. In our implants, CS inhibited the retraction observed in PRP clots and solid, voluminous CS/PRP implants increased stability in vivo, ensuring bioactivity for several weeks. Consistent with this hypothesis, CS/PRP implants have been shown to reside for several weeks in vivo and to possess significant bioactivity whereas recalcified PRP degraded in a day (Chevrier et al., 2017). In addition, when implanted subcutaneously, the sustained presence of CS/PRP implants induced cell recruitment and angiogenesis in the local milieu. A similar increase in recruitment of progenitor cells combined with increased angiogenesis will greatly influence the cartilage tissue regeneration and subchondral bone remodelling. In a previous study, cell number and density of progenitor-cell population available in cartilage defect following bone-marrow stimulation was found to be a vital factor impacting the eventual cartilage-repair outcome in a rabbit model (Dwivedi, Chevrier, Hoemann, & Buschmann, 2018).

Possibly through platelet activation, CS increases the concentration of bioactive factors including proangiogenic factors. Our own in-house data and other studies suggest that CS may stabilise platelets in PRP leading to sustained release of GFs (Deprés-Tremblay, Chevrier, Tran-Khanh, Nelea, & Buschmann, 2017). Kim et al had shown improved chondrocyte proliferation and matrix synthesis induced by sustained release of TGF-βI from CS scaffolds (Kim et al., 2003). Taken together, we believe that superior physical stability of CS/PRP implants leads to a significant increase in their biological activity arising from sustained residency and release of platelet-derived growth factors and inherent benefits of CS.

Potentiating effects of CS in articular cartilage healing has been demonstrated in multiple studies (Hsu et al., 2004; Lu, Prudhommeaux, Meunier, Sedel, & Guillemin, 1999; Mattioli-Belmonte et al., 1999; Risbud, Ringe, Bhonde, & Sittinger, 2001). Whereas CS helped in maintenance of morphology and ECM synthesis by chondrocytes in vitro (Hsu et al., 2004; Risbud et al., 2001), a thermosensitive CS gel promoted chondrogenic differentiation of BMSCs (Cho et al., 2004). CS has been shown to be chemotactic and increase recruitment and proliferation of BMSCs into defect (Chevrier et al., 2007), impede loss, and preserve viability of BMSCs (Busilacchi, Gigante, Mattioli-Belmonte, Manzotti, & Muzzarelli, 2013). Three-week analysis of repair tissues in our model revealed the presence of vascularised granulation tissue enriched with polymorphonuclear cells along with enlarged drill holes in CS/PRP group, similar to what was previously reported for CS-GP/blood implants (Chevrier et al., 2007; Guzman-Morales et al., 2014). In earlier studies, CS-GP/blood implants were found to stimulate a proangiogenic response in the granulation tissue. However, this proangiogenic response was transient and granulation tissue in the drill holes was eventually replaced by trabecular bone (Chevrier et al., 2007). A similar proangiogenic response was also observed in the microdrill holes of the rabbit treated with CS/PRP after 3 weeks in the current pilot study (Figure 3). Similar to our previous work, blood vessels were not observed in the chondral repair tissue at 8-week post-treatment with CS/PRP in the current main study, although blood vessels were certainly present underneath, in the marrow spaces of the bone plate and subchondral bone (Figure 6). Altogether, our data suggest that the CS/PRP implants induce transient angiogenesis in the subchondral compartment, although we would need to perform additional studies and sacrifice several animals at different early time points to properly investigate the mechanisms of action of the CS/PRP implants and draw solid conclusions.

In contrast, a typical fibrocartilagenous repair and endochondral ossification associated with hypertrophied chondrocytes and vascular invasion was observed in BMS only group, as previously reported (Chevrier et al., 2007; Shapiro et al., 1993). CS-GP/blood implants improve cartilage repair by, in part, increasing cell recruitment, vascularisation and bone remodelling, polarising the macrophage phenotype towards the alternatively-activated pro-wound healing lineage and stimulating secretion of anabolic wound repair factors (Chevrier et al., 2007; Hoemann et al., 2010; Chen et al., 2011; Guzman-Morales et al., 2014; Fong, Ariganello, Girard-Lauziere, & Hoemann, 2015). Wound-bloom effect as seen in previous studies was characterised by enhanced woven bone-plate repair in the drill holes along with increase in volume and hyaline quality of cartilage tissue, likely due to increased recruitment of chondrogenic stem cells to the cartilage lesion (Guzman-Morales et al., 2014). Here, we showed that CS/PRP implants appear to induce similar mechanisms. Taken together, these factors may drive the superior repair response in presence of CS/PRP implants indicated by more hyaline nature of repair accompanied by better macroscopic regeneration and increased bone remodelling. Because the cartilage repair outcome is strongly influenced by the properties of BMSCs including their number, proliferation, and chondrogenic potential (Dwivedi, Chevrier, Alameh, et al., 2018), application of CS/PRP is also likely to improve the cartilage repair outcome with poor prognosis arising due to low cell number or reduced chondrogenic potential in older patient population or patients with older defects.

One limitation of this study was its relatively short 8-week time point. Although increased hyaline nature of the repair tissue obtained with BMS + CS/PRP would be expected to provide long-term durability, this was not assessed here. In addition, we found high

interindividual variability in our results, which may arise due to immediate load bearing (Jubel et al., 2008) further compounded by small sample size used in this study. Nevertheless, in spite of these limitations, CS/PRP implants show promise in augmenting the beneficial effects of BMS in chronic models.

We believe that this study will motivate earnest reassessment of preclinical cartilage-repair models. Because prompt diagnosis and treatment of cartilage defects is rare, approaches aimed at improving repair in presence of altered joint hemostasis is warranted. The chronic model studied here is more comparable with human chronic defects than the corresponding acute model. Our results show promising results in unveiling the positive role of CS/PRP implants for improvement of BMS mediated cartilage repair in chronic defects. In the future, a larger study with increased duration of repair and additional control groups will be undertaken to shed more light on the underlying mechanism of inflammatory and metabolic changes accompanying pathogenesis and repair of chronic defects using CS/PRP implants.

ACKNOWLEDGEMENTS

We acknowledge the technical contributions of Jun Sun and Geneviève Picard. This work was supported by the Canadian Institutes of Health Research, Canada Foundation for Innovation, Groupe de Recherche en Sciences et Technologies Biomédicales, Natural Sciences and Engineering Research Council of Canada, and Ortho Regenerative Technologies Inc.

CONFLICT OF INTEREST

AC, CDH and MDB hold shares, CDH and MDB are Directors of Ortho Regenerative Technologies Inc.

DISCLOSURES

A. C., C. D. H., and M. D. B. hold shares and C. D. H. and M. D. B. are Directors of Ortho Regenerative Technologies Inc.

AUTHOR CONTRIBUTIONS

The following authors contributed to the conception and design of the study (G. D., A. C., C. D. H., and M. D. B.), acquisition of data (G. D. and A. C.), analysis and interpretation of the data (G. D., A. C., C. D. H., and M. D. B.) drafting the article and revising (G. D., A. C., C. D. H., and M. D. B.), final approval of the manuscript (M. D. B.).

ORCID

Michael D. Buschmann https://orcid.org/0000-0001-7555-8189

REFERENCES

Bouwmeester, P., Kuijer, R., Terwindt-Rouwenhorst, E., van der Linden, T., & Bulstra, S. (1999). Histological and biochemical evaluation of perichondrial transplants in human articular cartilage defects. *Journal of Orthopaedic Research*, *17*(6), 843–849. https://doi.org/10.1002/jor.1100170609

Bouwmeester, P. S., Kuijer, R., Homminga, G. N., Bulstra, S. K., & Geesink, R. G. (2002). A retrospective analysis of two independent prospective cartilage repair studies: Autogenous perichondrial grafting versus subchondral drilling 10 years post-surgery. *Journal of Orthopaedic Research*, *20*(2), 267–273. https://doi.org/10.1016/S0736-0266(01)00099-7

Bredella, M. A., Tirman, P. F., Peterfy, C. G., Zarlingo, M., Feller, J. F., Bost, F. W., … Genant, H. K. (1999). Accuracy of T2-weighted fast spin-echo MR imaging with fat saturation in detecting cartilage defects in the knee: Comparison with arthroscopy in 130 patients. *American Journal of Roentgenology*, *172*(4), 1073–1080. https://doi.org/10.2214/ajr.172.4.10587150

Brehm, W., Aklin, B., Yamashita, T., Rieser, F., Trub, T., Jakob, R. P., & Mainil-Varlet, P. (2006). Repair of superficial osteochondral defects with an autologous scaffold-free cartilage construct in a caprine model: Implantation method and short-term results. *Osteoarthritis Cartilage*, *14*(12), 1214–1226. https://doi.org/10.1016/j.joca.2006.05.002

Busilacchi, A., Gigante, A., Mattioli-Belmonte, M., Manzotti, S., & Muzzarelli, R. A. A. (2013). Chitosan stabilizes platelet growth factors and modulates stem cell differentiation toward tissue regeneration. *Carbohydrate Polymers*, *98*(1), 665–676. https://doi.org/10.1016/j.carbpol.2013.06.044

Chen, G., Sun, J., Lascau-Coman, V., Chevrier, A., Marchand, C., & Hoemann, C. D. (2011). Acute osteoclast activity following subchondral drilling is promoted by chitosan and associated with improved cartilage repair tissue integration. *Cartilage*, *2*(2), 173–185. https://doi.org/10.1177/1947603510381096

Chen, H., Chevrier, A., Hoemann, C. D., Sun, J., Picard, G., & Buschmann, M. D. (2013). Bone marrow stimulation of the medial femoral condyle produces inferior cartilage and bone repair compared to the trochlea in a rabbit surgical model. *Journal of Orthopaedic Research*, *31*(11), 1757–1764. https://doi.org/10.1002/jor.22422

Chen, H., Hoemann, C. D., Sun, J., Chevrier, A., McKee, M. D., Shive, M. S., … Buschmann, M. D. (2011). Depth of subchondral perforation influences the outcome of bone marrow stimulation cartilage repair. *Journal of Orthopaedic Research*, *29*(8), 1178–1184. https://doi.org/10.1002/jor.21386

Chen, H., Sun, J., Hoemann, C. D., Lascau-Coman, V., Wei, O., McKee, M. D., … Buschmann, M. D. (2009). Drilling and microfracture lead to different bone structure and necrosis during bone-marrow stimulation for cartilage repair. *Journal of Orthopaedic Research*, *27*(11), 1432–1438. https://doi.org/10.1002/jor.20905

Chevrier, A., Darras, V., Picard, G., Nelea, M., Veilleux, D., Lavertu, M., … Buschmann, M. D. (2017). Injectable chitosan-platelet-rich plasma (PRP) implants to promote tissue regeneration: In vitro properties, in vivo residence, degradation, cell recruitment and vascularization. *Journal of Tissue Engineering and Regenerative Medicine*, *12*(1), 217–228. https://doi.org/10.1002/term.2403

Chevrier, A., Hoemann, C. D., Sun, J., & Buschmann, M. D. (2007). Chitosan-glycerol phosphate/blood implants increase cell recruitment, transient vascularization and subchondral bone remodeling in drilled cartilage defects. *Osteoarthritis and Cartilage*, *15*(3), 316–327. https://doi.org/10.1016/j.joca.2006.08.007

Cho, J. H., Kim, S. H., Park, K. D., Jung, M. C., Yang, W. I., Han, S. W., … Lee, J. W. (2004). Chondrogenic differentiation of human mesenchymal stem cells using a thermosensitive poly(N-isopropylacrylamide) and water-soluble chitosan copolymer. *Biomaterials*, *25*(26), 5743–5751. https://doi.org/10.1016/j.biomaterials.2004.01.051

Deprés-Tremblay, G., Chevrier, A., Tran-Khanh, N., Nelea, M., & Buschmann, M. (2017). Chitosan inhibits platelet-mediated clot retraction, increases platelet-derived growth factor release, and increases residence time and bioactivity of platelet-rich plasma in vivo. *Biomedical Materials*, *13*(1), 015005. https://doi.org/10.1088/1748-605X/aa8469

Drengk, A., Zapf, A., Sturmer, E. K., Sturmer, K. M., & Frosch, K. H. (2009). Influence of platelet-rich plasma on chondrogenic differentiation and

proliferation of chondrocytes and mesenchymal stem cells. *Cells, Tissues, Organs*, *189*(5), 317–326. https://doi.org/10.1159/000151290

Dwivedi, G., Chevrier, A., Alameh, M. G., Hoemann, C. D., & Buschmann, M. D. (2018). Quality of cartilage repair from marrow stimulation correlates with cell number, clonogenic, chondrogenic and matrix production potential of underlying bone marrow stromal cells in a rabbit model. *Cartilage*. In Press, DOI: https://doi.org/10.1177/1947603518812555

Dwivedi, G., Chevrier, A., Hoemann, C. D., & Buschmann, M. D. (2018). Bone marrow progenitor cells isolated from young rabbit trochlea are more numerous and exhibit greater clonogenic, chondrogenic and osteogenic potential than cells isolated from condyles. *Cartilage*, *9*(4), 378–390. https://doi.org/10.1177/1947603517693044

Fong, D., Ariganello, M. B., Girard-Lauziere, J., & Hoemann, C. D. (2015). Biodegradable chitosan microparticles induce delayed STAT-1 activation and lead to distinct cytokine responses in differentially polarized human macrophages in vitro. *Acta Biomaterialia*, *12*, 183–194. https://doi.org/10.1016/j.actbio.2014.10.026

Gaissmaier, C., Fritz, J., Krackhardt, T., Flesch, I., Aicher, W. K., & Ashammakhi, N. (2005). Effect of human platelet supernatant on proliferation and matrix synthesis of human articular chondrocytes in monolayer and three-dimensional alginate cultures. *Biomaterials*, *26*(14), 1953–1960. https://doi.org/10.1016/j.biomaterials.2004.06.031

Gonshor, A. (2002). Technique for producing platelet-rich plasma and platelet concentrate: background and process. *The International Journal of Periodontics & Restorative Dentistry*, *22*(6), 547–557.

Guzman-Morales, J., Lafantaisie-Favreau, C. H., Chen, G., & Hoemann, C. D. (2014). Subchondral chitosan/blood implant-guided bone plate resorption and woven bone repair is coupled to hyaline cartilage regeneration from microdrill holes in aged rabbit knees. *Osteoarthritis and Cartilage*, *22*(2), 323–333. https://doi.org/10.1016/j.joca.2013.12.011

Harada, Y., Nakasa, T., Mahmoud, E. E., Kamei, G., Adachi, N., Deie, M., & Ochi, M. (2015). Combination therapy with intra-articular injection of mesenchymal stem cells and articulated joint distraction for repair of a chronic osteochondral defect in the rabbit. *Journal of Orthopaedic Research*, *33*(10), 1466–1473. https://doi.org/10.1002/jor.22922

Hardaker, W. T. Jr., Garrett, W. E. Jr., & Bassett, F. H. III (1990). Evaluation of acute traumatic hemarthrosis of the knee joint. *Southern Medical Journal*, *83*(6), 640–644. https://doi.org/10.1097/00007611-199006000-00011

Hepp, P., Osterhoff, G., Niederhagen, M., Marquass, B., Aigner, T., Bader, A., … Schulz, R. (2009). Perilesional changes of focal osteochondral defects in an ovine model and their relevance to human osteochondral injuries. *Journal of Bone and Joint Surgery (British)*, *91*(8), 1110–1119.

Hoemann, C. D., Chen, G., Marchand, C., Tran-Khanh, N., Thibault, M., Chevrier, A., … El-Gabalawy, H. (2010). Scaffold-guided subchondral bone repair implication of neutrophils and alternatively activated arginase-1+macrophages. *The American Journal of Sports Medicine*, *38*(9), 1845–1856. https://doi.org/10.1177/0363546510369547

Hoemann, C. D., Hurtig, M., Rossomacha, E., Sun, J., Chevrier, A., Shive, M., & Buschmann, M. (2005). Chitosan-glycerol phosphate/blood implants improve hyaline cartilage repair in ovine microfracture defects. *The Journal of Bone and Joint Surgery. American Volume*, *87A*(12), 2671–2686.

Hoemann, C. D., Sun, J., McKee, M. D., Chevrier, A., Rossomacha, E., Rivard, G. E., … Buschmann, M. D. (2007). Chitosan-glycerol phosphate/blood implants elicit hyaline cartilage repair integrated with porous subchondral bone in microdrilled rabbit defects. *Osteoarthritis and Cartilage*, *15*(1), 78–89. https://doi.org/10.1016/j.joca.2006.06.015

Hoemann, C. D., Tran-Khanh, N., Chevrier, A., Chen, G., Lascau-Coman, V., Mathieu, C., … Buschmann, M. D. (2015). Chondroinduction is the main cartilage repair response to microfracture and microfracture with BST-CarGel: Results as shown by ICRS-II histological scoring and a novel zonal collagen type scoring method of human clinical biopsy specimens. *The American Journal of Sports Medicine*, *43*(10), 2469–2480. https://doi.org/10.1177/0363546515593943

Hsu, S. H., Whu, S. W., Hsieh, S. C., Tsai, C. L., Chen, D. C., & Tan, T. S. (2004). Evaluation of chitosan-alginate-hyaluronate complexes modified by an RGD-containing protein as tissue-engineering scaffolds for cartilage regeneration. *Artificial Organs*, *28*(8), 693–703. https://doi.org/10.1111/j.1525-1594.2004.00046.x

Hunziker, E. B. (1999). Biologic repair of articular cartilage. Defect models in experimental animals and matrix requirements. *Clinical Orthopaedics and Related Research*, *367* Suppl, S135–S146. https://doi.org/10.1097/00003086-199910001-00015

Jubel, A., Andermahr, J., Schiffer, G., Fischer, J., Rehm, K. E., Stoddart, M. J., & Hauselmann, H. J. (2008). Transplantation of de novo scaffold-free cartilage implants into sheep knee chondral defects. *The American Journal of Sports Medicine*, *36*(8), 1555–1564. https://doi.org/10.1177/0363546508321474

Kaps, C., Loch, A., Haisch, A., Smolian, H., Burmester, G. R., Haupl, T., & Sittinger, M. (2002). Human platelet supernatant promotes proliferation but not differentiation of articular chondrocytes. *Medical & Biological Engineering & Computing*, *40*(4), 485–490. https://doi.org/10.1007/BF02345083

Kim, S. E., Park, J. H., Cho, Y. W., Chung, H., Jeong, S. Y., Lee, E. B., & Kwon, I. C. (2003). Porous chitosan scaffold containing microspheres loaded with transforming growth factor-beta1: Implications for cartilage tissue engineering. *Journal of Controlled Release*, *91*(3), 365–374. https://doi.org/10.1016/S0168-3659(03)00274-8

Kon, E., Filardo, G., Delcogliano, M., Fini, M., Salamanna, F., Giavaresi, G., … Marcacci, M. (2010). Platelet autologous growth factors decrease the osteochondral regeneration capability of a collagen-hydroxyapatite scaffold in a sheep model. *BMC Musculoskeletal Disorders*, *11*, 220. https://doi.org/10.1186/1471-2474-11-220

Kruger, J. P., Hondke, S., Endres, M., Pruss, A., Siclari, A., & Kaps, C. (2012). Human platelet-rich plasma stimulates migration and chondrogenic differentiation of human subchondral progenitor cells. *Journal of Orthopaedic Research*, *30*(6), 845–852. https://doi.org/10.1002/jor.22005

Lavertu, M., Xia, Z., Serreqi, A. N., Berrada, M., Rodrigues, A., Wang, D., … Gupta, A. (2003). A validated 1H NMR method for the determination of the degree of deacetylation of chitosan. *Journal of Pharmaceutical and Biomedical Analysis*, *32*(6), 1149–1158. https://doi.org/10.1016/S0731-7085(03)00155-9

Lee, H.-R., Park, K. M., Joung, Y. K., Park, K. D., & Do, S. H. (2012). Platelet-rich plasma loaded hydrogel scaffold enhances chondrogenic differentiation and maturation with up-regulation of CB1 and CB2. *Journal of Controlled Release*, *159*(3), 332–337. https://doi.org/10.1016/j.jconrel.2012.02.008

Li, H., Usas, A., Poddar, M., Chen, C. W., Thompson, S., Ahani, B., … Huard, J. (2013). Platelet-rich plasma promotes the proliferation of human muscle derived progenitor cells and maintains their stemness. *PLoS ONE*, *8*(6), e64923. https://doi.org/10.1371/journal.pone.0064923

Lu, J. X., Prudhommeaux, F., Meunier, A., Sedel, L., & Guillemin, G. (1999). Effects of chitosan on rat knee cartilages. *Biomaterials*, *20*(20), 1937–1944.

Marchand, C., Chen, H., Buschmann, M. D., & Hoemann, C. D. (2011). Standardized three-dimensional volumes of interest with adapted surfaces for more precise subchondral bone analyses by micro-computed tomography. *Tissue Engineering Part C*, *17*(4), 475–484. https://doi.org/10.1089/ten.tec.2010.0417

Marx, R. E. (2001). Platelet-rich plasma (PRP): What is PRP and what is not PRP? *Implant Dentistry*, *10*(4), 225–228. https://doi.org/10.1097/00008505-200110000-00002

Marx, R. E., Carlson, E. R., Eichstaedt, R. M., Schimmele, S. R., Strauss, J. E., & Georgeff, K. R. (1998). Platelet-rich plasma: Growth factor enhancement for bone grafts. *Oral Surgery, Oral Medicine, Oral Pathology, Oral Radiology, and Endodontics*, *85*(6), 638–646. https://doi.org/10.1016/S1079-2104(98)90029-4

Mattioli-Belmonte, M., Gigante, A., Muzzarelli, R. A., Politano, R., De Benedittis, A., Specchia, N., … Greco, F. (1999). N,N-dicarboxymethyl chitosan as delivery agent for bone morphogenetic protein in the repair of articular cartilage. *Medical & Biological Engineering & Computing*, *37*(1), 130–134. https://doi.org/10.1007/BF02513279

Milano, G., Sanna Passino, E., Deriu, L., Careddu, G., Manunta, L., Manunta, A., … Fabbriciani, C. (2010). The effect of platelet rich plasma combined with microfractures on the treatment of chondral defects: An experimental study in a sheep model. *Osteoarthritis and Cartilage*, *18*(7), 971–980. https://doi.org/10.1016/j.joca.2010.03.013

Mizuta, H., Kudo, S., Nakamura, E., Takagi, K., & Hiraki, Y. (2006). Expression of the PTH/PTHrP receptor in chondrogenic cells during the repair of full-thickness defects of articular cartilage. *Osteoarthritis and Cartilage*, *14*(9), 944–952. https://doi.org/10.1016/j.joca.2006.03.009

Nguyen, S., Winnik, F. M., & Buschmann, M. D. (2009). Improved reproducibility in the determination of the molecular weight of chitosan by analytical size exclusion chromatography. *Carbohydrate Polymers*, *75*(3), 528–533. https://doi.org/10.1016/j.carbpol.2008.08.013

Park, S. I., Lee, H. R., Kim, S., Ahn, M. W., & Do, S. H. (2012). Time-sequential modulation in expression of growth factors from platelet-rich plasma (PRP) on the chondrocyte cultures. *Molecular and Cellular Biochemistry*, *361*(1–2), 9–17. https://doi.org/10.1007/s11010-011-1081-1

Risbud, M., Ringe, J., Bhonde, R., & Sittinger, M. (2001). In vitro expression of cartilage-specific markers by chondrocytes on a biocompatible hydrogel: Implications for engineering cartilage tissue. *Cell Transplantation*, *10*(8), 755–763. https://doi.org/10.3727/000000001783986224

Rodrigo, J. J., Steadman, J. R., Syftestad, G., Benton, H., & Silliman, J. (1995). Effects of human knee synovial fluid on chondrogenesis in vitro. *The American Journal of Knee Surgery*, *8*(4), 124–129.

Saris, D. B., Dhert, W. J., & Verbout, A. J. (2003). Joint homeostasis. The discrepancy between old and fresh defects in cartilage repair. *Journal of Bone and Joint Surgery (British)*, *85*(7), 1067–1076.

Shapiro, F., Koide, S., & Glimcher, M. J. (1993). Cell origin and differentiation in the repair of full-thickness defects of articular cartilage. *The Journal of Bone and Joint Surgery. American Volume*, *75*(4), 532–553. https://doi.org/10.2106/00004623-199304000-00009

Shive, M. S., Stanish, W. D., McCormack, R., Forriol, F., Mohtadi, N., Pelet, S., … Restrepo, A. (2015). BST-CarGel(R) treatment maintains cartilage repair superiority over microfracture at 5 years in a multicenter randomized controlled trial. *Cartilage*, *6*(2), 62–72. https://doi.org/10.1177/1947603514562064

Simpson, A. H., Mills, L., & Noble, B. (2006). The role of growth factors and related agents in accelerating fracture healing. *Journal of Bone and Joint Surgery (British)*, *88*(6), 701–705.

Smyth, N. A., Murawski, C. D., Fortier, L. A., Cole, B. J., & Kennedy, J. G. (2013). Platelet-rich plasma in the pathologic processes of cartilage: Review of basic science evidence. *arthroscopy*, *29*(8), 1399–1409. https://doi.org/10.1016/j.arthro.2013.03.004

Stanish, W. D., McCormack, R. G., Forriol, F., Mohtadi, N., Pelet, S., Desnoyers, J., … Shive, M. S. (2013). Novel scaffold-based BST-CarGel treatment results in superior cartilage repair compared with microfracture in a randomized controlled trial. *The Journal of Bone and Joint Surgery. American Volume*, *95A*(18), 1640–1650.

van den Borne, M. P., Raijmakers, N. J., Vanlauwe, J., Victor, J., de Jong, S. N., Bellemans, J., & Saris, D. B. (2007). International Cartilage Repair Society (ICRS) and oswestry macroscopic cartilage evaluation scores validated for use in autologous chondrocyte implantation (aci) and microfracture. *Osteoarthritis and Cartilage*, *15*(12), 1397–1402. https://doi.org/10.1016/j.joca.2007.05.005

Varum, K. M., Ottoy, M. H., & Smidsrod, O. (2001). Acid hydrolysis of chitosans. *Carbohydrate Polymers*, *46*(1), 89–98. https://doi.org/10.1016/S0144-8617(00)00288-5

Veillette, C. J., & McKee, M. D. (2007). Growth factors—BMPs, DBMs, and buffy coat products: Are there any proven differences amongst them? *Injury*, *38*(Suppl 1), S38–S48. https://doi.org/10.1016/j.injury.2007.02.009

Verbruggen, G., Wittoek, R., Groeneboer, S., Cruyssen, B. V., Goemaere, S., & Elewaut, D. (2007). Osteochondral repair in synovial joints. *Current Opinion in Rheumatology*, *19*(3), 265–271. https://doi.org/10.1097/BOR.0b013e3280be58ff

SUPPORTING INFORMATION

Additional supporting information may be found online in the Supporting Information section at the end of the article.

Figure S1 (a-f): Assessment of 8-week repair outcome in subchondral bone of 4 week old chronic defects treated with BMS + PRP or BMS + CS/PRP—MicroCT 3-D analysis showed differences in structural parameters between defects treated with BMS + CS/PRP versus defects treated with BMS + PRP. Although the results were not significant, the values for bone surface density (a), bone surface (b), connectivity density (c), and trabecular number (f) were trending high for BMS + CS/PRP group versus BMS + PRP group, suggesting an increase in bone remodeling. (i). Schematic representing the region of interest (ROI) for micro CT analysis.

How to cite this article: Dwivedi G, Chevrier A, Hoemann CD, Buschmann MD. Injectable freeze-dried chitosan-platelet-rich-plasma implants improve marrow-stimulated cartilage repair in a chronic-defect rabbit model. *J Tissue Eng Regen Med*. 2019;1–13. https://doi.org/10.1002/term.2814